Application of modified green algae Nannochloropsis sp. as adsorbent in the simultaneous adsorption of methylene blue and Cu(II) cations in solution

Buhani (buhani_s@yahoo.co.id)
University Lampung https://orcid.org/0000-0003-2289-1804
Tri Agus Wijayanti
Universitas Lampung
Suharso
Universitas Lampung
Sumadi
Universitas Lampung
Muslim Ansori
Lampung University: Universitas Lampung

Research

Keywords: Nannochloropsis sp, algae-silica-magnetite hybrid, adsorption, methylene blue, heavy metal, Cu(II) cation

Posted Date: February 1st, 2021

DOI: https://doi.org/10.21203/rs.3.rs-64063/v2

Version of Record: A version of this preprint was published at Sustainable Environment Research on April 23rd, 2021. See the published version at https://doi.org/10.1186/s42834-021-00090-y.

Application of modified green algae *Nannochloropsis* sp. as adsorbent in the simultaneous adsorption of methylene blue and Cu(II) cations in solution

Buhani[1]*, Tri Agus Wijayanti[1], Suharso[1]*, Sumadi[2], Muslim Ansori[3]

[1]Department of Chemistry, University of Lampung, Bandar Lampung 35145, Indonesia

[2]Department of Electrical Engineering, University of Lampung, Bandar Lampung 35145, Indonesia

[3]Department of Mathematics, University of Lampung, Bandar Lampung 35145, Indonesia

*Correspondence: buhani_s@yahoo.co.id; suharso_s@yahoo.com

Abstract

Biomass of algae is a very potent adsorbent for absorbing liquid waste containing heavy metals and organic dyes. This study purposes to confirm the ability of adsorbents from green algae *Nannochloropsis* sp. modified with silica (ASN) and followed by coating magnetite particles (ASN-MPs) to absorb simultaneously the mixture of methylene blue (ME) and Cu(II) cations in aqueous solution. Simultaneous sorption of ME and Cu(II) cations to ASN and ASN-MPs was carried out by the Batch method with the interaction pH condition 7, contact time 90 minutes, and initial concentrations of ME and Cu(II) cations (0.1 - 1.0 mmol L^{-1}). Based on adsorption data, Cu(II) cations have a greater adsorption rate and capacity (q_m) compared to ME at the same contact time and initial concentration. The adsorption capacity (q_m) values of the bi-component ME and Cu(II) cation mixture in ASN and ASN-MPs were 1.385 x 10^{-1} and 5,319 x 10^{-1} mmolequiv g^{-1}, respectively, with the binary Langmuir adsorption isotherm constant for Cu(II) cations greater than ME. Modified adsorbent from algae *Nannochloropsis* sp. with silica matrix and magnetite particle coating, is an adsorbent that has a high effectiveness in the collective sorption of ME and Cu(II) cations. Therefore, these adsorbents can be used for the adsorption of cation mixtures of heavy

metals and organic dyes that are cationic in solution.

Keywords: *Nannochloropsis* sp; algae-silica-magnetite hybrid; adsorption; methylene blue, heavy metal, Cu(II) cation.

1. Introduction

Organic dyes and heavy metals are sources of pollutants that are often found in the environment, especially in waters. Heavy metals and dyes are produced from by-products or various industrial wastes such as textiles and petrochemicals. Heavy metals such as Cu exposed to the environment can come from electroplating plants, mining, industrial, and municipal wastes [1] while organic dyes such as methylene blue (ME) are applied considerably as agents of dyes in varied industry such as the pharmaceutical, leather, paper and textile industries [2]. Because of this, the presence of these toxic chemicals needs to be reduced from the environment so that they do not have a negative impact on human health and the surrounding environment.

At present, several methods have been developed to reduce pollution from liquid waste in the form of physicochemical technology including ion exchange, coagulation, flocculation, chemical oxidation, electrochemical techniques, membrane separation, adsorption, and photocatalysis which have been applied for the purpose of removing

54 dyes and metal ions from waste water [3-9]. From some of these technologies, the
55 adsorption method is more often used for the treatment of liquid waste containing heavy
56 metals or hazardous dyes. This is done with the consideration that the process of
57 adsorption method is really easy, the cost applied is not expensive, and it is safe for the
58 environment [10]. Sorption processes typically use adsorbents derived from the
59 synthesis or modified natural material.

60 Currently, various adsorbents have been developed from natural materials for waste
61 treatment before being discharged into the environment, such as algal biomass.
62 Biomass from algae is originally a very potent adsorbent to absorb pollutants of
63 inorganic materials like heavy metals [11-13] and organic materials originated from
64 toxic dye agents [14,15]. Algal biomass has a great potential to bind dyes, especially
65 organic dyes in the form of cations as well as metal ions. Several studies have shown
66 that live algae and its biomass may absorb organic cations and metal ions [16,17].
67 Adsorption of metal ions and dyes on algal biomass occurs through reaction
68 mechanisms involving the contribution of active groups of proteins, polysaccharides,
69 and functional groups like hydroxyl, amino, sulfate ions, carboxyl, etc. [18, 19].

70 However, the ability of algae to bind these chemical compounds is very limited by

several constraints such as small size, low density and easily damaged due to degradation by other microorganisms [20]. In addition, algae cannot be used directly in the adsorption column, because it is very soft and is not granular [9]. To increase the capacity and rate of algal adsorption on adsorbents absorbed as well as physical and chemical stability, various attempts were made including modifying algal biomass using various supporting matrix in the form of inorganic and organic materials [2,18]. Materials produced from inorganic-organic hybrids, such as algal-silica hybrids, are very promising substances for poisonous dye and heavy metal ion adsorbents [21-24].

The physical and chemical quality of adsorbents derived from algae were able to be performed by employing the sol-gel process in making adsorbents with silica support matrices, because these processes produce homogeneous adsorbents [25-28]. In addition, a rising in the sorption rate of the adsorbate was able to be carried out using magnetite particle coating techniques [29-31]. The adsorbent coating technique by particles of magnetite is safe for environment, since it does not produce side products that conceive contamination like suspended solids, besides that it also accelerates the process of isolating the adsorbate from the solution caused by the magnetic properties of the adsorbent [32-34]. By using the adsorbent coating technique using magnetite

88 particles, we will get an adsorbent with a big adsorption rate and capacity to the
89 adsorbate, so that the adsorption process becomes more efficient.

90 In a waste treatment system, multicomponent mixtures are often found, namely the
91 presence of various types of chemical compounds both inorganic and organic
92 compounds, therefore it is necessary to develop an adsorbent that is not only effective
93 at absorbing heavy metals, but also effective against other compounds such as dyes
94 contained in the mixture from ME. Therefore, the purpose of this work is to learn the
95 competition for sorption of a mixture of ME and Cu(II) cations in solution on modified
96 *Nannochloropsis* sp. (algae-silica-magnetite). The adsorbents used in this study have
97 complex chemical and biological compositions, so it is very interesting to study from a
98 theoretical and experimental point of view in their application as a material for
99 absorbing dyes and metal ions in solution. Biomass from *Nannochloropsis* sp. algae
100 has been modified with silica followed by coating with magnetite (Fe_3O_4) particles
101 utilized as an effective and cheaper adsorbent to separate ME and Cu(II) cations
102 simultaneously from the solution. The adsorption competition between ME and Cu(II)
103 cations in ASN-MPs adsorbents was studied with a series of batch experiments
104 including: variations in contact time, initial concentration, sequential desorption, and

105 re-use of adsorbent tests. Simultaneous adsorption kinetics and isotherm parameters as
106 well as their mechanism are confirmed to predict the sorption properties of ME and
107 Cu(II) cations by ASN-MPs.

108 **2. Materials and methods**

109 *2.1. Materials*

110 The used materials in this work include *Nannochloropsis* sp. algae originating
111 from Balai Besar Budidaya Laut Lampung (the Lampung Sea Cultivation Bureau),
112 Republic of Indonesia. The used chemicals were obtained from European
113 Pharmacopoeia consisting of: tetraethyl orthosilicate (TEOS), $FeSO_4 \cdot 4H_2O$,
114 $FeCl_3 \cdot 6H_2O$, HCl, NaOH, ethanol, methylene blue (ME), $CuSO_4 \cdot 5H_2O$, and Na_2EDTA.
115 Magnetite particles were synthesized according to the procedure by Buhani *et al* [11].
116 Stocks of ME dye and $CuSO_4 \cdot 5H_2O$ solutions were each prepared with a concentration
117 of 1000 mmol L^{-1} which was used as standard solution and adsorbate. All the
118 experiments in this study used double distilled water.

119 *2.2. Preparation of adsorbent and materials: Nannochloropsis* sp., *ASN, and ASN-MPs*

120 *Nannochloropsis* sp. algae were neutralized (up to neutral pH) by rinsing with
121 water, then dried for 3 days with air dry. The algae biomass was then placed at 40 ºC

for 2-3 hours then crushed using a 100 mesh grinder. The *Nannochloropsis* sp. algae biomass was used to make ASN-MPs adsorbents in the following way: a total of 5.0 mL of TEOS and 2.5 mL of deionized water was mixed into a plastic bottle, then gained 0.1 g magnetite. The mixture was stirred for 30 minutes using a magnetic stirrer. When stirring, the pH of the solution was made to be pH of 2 with the addition of 1 M HCl by dropwise. In another bottle, *Nannochloropsis* sp. biomass (0.4 g) and ethanol (5 mL) were mixed by a magnetic stirrer for 30 minutes. Then, the two solutions were mixed while stirring until the mixture turns into a gel. The formed gel was filtered with filter paper and allowed for 24 hours. The gel was afterward rinsed using deionized water and ethanol with a ratio of 60/40 to pH≈7. Furthermore, the gel was placed in the oven to be dried at 40 ºC for 2-3 hours and crushed using a grinder until smooth with a size of 100 mesh.

2.3. Characterization of ASN and ASN-MPs adsorbent

The ASN adsorbents and ASN-MPs were investigated by Fourier-transform infrared spectroscopy (FTIR) to recognize specific functional groups contained (Shimadzu Prestige-21 IR, Japan). The adsorbent crystallinity level was analyzed by XRD (Shimadzu 6000, Japan). The distribution of particle size from material was also

139 investigated by the particle size analyzer (Fritsch Analysette 22). Surface
140 morphological analysis and element constituents were performed using Scanning
141 Electron Microscopy with Energy Dispersive X-Ray (SEM-EDX) (Zeiss MA10,
142 Germany.

143 *2.4. Adsorption experiments*

144 The experimental procedure to study the adsorption competition ME and Cu(II)
145 cations was carried out under the following adsorption conditions: a dose of 0.1 g
146 adsorbent was used in a batch system controlled by a shaker (Stuart reciprocating
147 shaker SSL2), the sorption process was held at 27 ºC, interaction pH was 7, and an
148 adsorbate volume was 50 mL. The adsorption kinetics of ME and Cu(II) cations in
149 the mixture were studied with varying contact times between 15-120 minutes. The
150 adsorption rate was determined based on the pseudo first order kinetics (Eq. (4)) and
151 the pseudo second order kinetics (Eq. (5)) and the intra-particle diffusion pattern (IPD)
152 was analyzed using (Eq. (6)). For the simultaneous adsorption experiment, each
153 solution of ME and Cu(II) cation at the similar concentration (between 0.1 - 1.0 mmol
154 L^{-1}) was mixed with the optimum contact time. The simultaneous adsorption isotherm
155 pattern of ME and Cu(II) cation was determined using the Langmuir adsorption

156 isotherm equation (Eq. (7)), Freundlich (Eq. (8)), and the Langmuir isotherm equation
157 for a binary mixture (Eq. (9)). The adsorption experiment was carried out in 3 times
158 of parallel repetitions. UV-Vis spectrophotometer (Agilent Cary 100, U.S.A) was
159 performed to analyze the concentrations of ME adsorbed on the adsorbent at a
160 maximum wavelength of 664 nm. The concentrations of Cu(II) cations adsorbed by the
161 adsorbent were tested with atomic absorption spectrophotometer (AAS) (Perkins Elmer
162 3110, U.S.A).

163 The Equations (Eqs. (1), (2), and (3)) were used to determine an amount of
164 adsorbed ME or Cu(II) cations per unit mass of adsorbent and the percentage of
165 adsorbed ME or Cu(II) cations.

166 $$q_e = \frac{(C_o - C_e)}{m} xV \quad (1)$$

167 $$q_t = \frac{(C_o - C_t)}{m} xV \quad (2)$$

168 $$R(\%) = \frac{(C_o - C_t)}{C_o} x100 \quad (3)$$

169 Concentrations (mmol L^{-1}) of ME or Cu(II) cation solution at initial state, equilibrium,
170 and certain time of t were expressed as C_o, C_e, and C_t, respectively. The mass of
171 adsorbent (g), the volume of the solution (L), the amount of ME or Cu(II) cations
172 adsorbed per unit mass (mmol g^{-1}), and the percentage of the ME or Cu(II) cation

adsorption are expressed by m, V, q, and R, respectively.

2.4. Sequential desorption

To find out the type of interaction between ASN-MPs adsorbents with ME or Cu(II) cations , a sequential desorption experiment was conducted as follows: 0.1 g of ASN-MPs adsorbents were added to each ME or Cu(II) cation at conditions (pH = 7, T = 27 °C, t = 90 minutes, volume = 50 mL, and adsorbate concentration 0.1 mmol L^{-1}). Adsorbates adsorbed on the AS-MPs adsorbent were sequentially released using several eluents such as aquades, HCl (0.1 M), and Na_2EDTA (0.1 M).

2.5. Reusability of adsorbent

The ability to reuse adsorbents was studied by performing the adsorption process singly at the optimum condition (adsorbent dosage = 0.1 g, pH = 7, T = 27 °C, t = 90 minutes, volume = 50 mL, and adsorbate concentration 0.1 mmol L^{-1}). The adsorbate adsorbed was eluted by an eluent of 0.1 M HCl (50 mL). Then, the distilled water was used to rinse the adsorbent to reach neutral pH. The adsorption-desoption process was repeated several times, up to % adsorption from ME or Cu(II) cations < 80%.

3. Results and discussion

3.1. Characterization of ASN and ASN-MPs adsorbent

To find out the success of the modification process of *Nannochloropsis* sp. algae using silica matrix and magnetite particle coating, identification of the adsorbent functional groups was carried out using FTIR. In ASN adsorbents (Fig. 1b) and ASN-MPs (Fig.1c), there is a relatively similar IR absorption with the appearance of absorption bands at wave numbers around 794.8-784.3 cm^{-1} originating from Si-O-Si and 482.9-432.9 cm^{-1} of the Si-O stretching vibrations (siloxan groups) derived from silica as a matrix. The contribution of *Nannochloropsis* sp. algae to ASN and ASN-MPs is indicated by the appearance of absorption bands in the region of wave number 2931.80 cm^{-1} originating from C-H stretching vibration absorption from (-CH_2) aliphatic as shown in Fig. 1a. In addition, absorption bands were seen in wave numbers 3448.72-3442.72 cm^{-1} originating from hydroxyl groups (-OH) and 1658.78-1651.07 cm^{-1} (carbonyl groups). This shows that there has been a hybridization between *Nannochloropsis* sp. and silica matrix. The presence of magnetite particles in ASN and ASN-MPs could not be observed through FTIR spectrum. In addition, the absence of absorption in the area of wave number 964.41 cm^{-1} indicating the stretching vibration

207 of silanol (Si-OH) on the ASN-MPs adsorbent (Fig. 1c) as shown in the ASN spectrum
208 (Fig. 1b) indicates that there has been an interaction between the silanol groups and the
209 magnetite particles. The presence of magnetite particles in ASN-MPs is strengthened
210 from the results of the EDX spectrum [11].

211 Fig. 2 displays the morphology of ASN (Fig. 2a) showing an agglomeration
212 originating from the amorphous silica matrix and *Nannochloropsis* sp., this is supported
213 by elemental constituent data from the analysis of EDX on ASN (Fig. 2c) consisting of
214 Si, O, C, and N. The ASN-MPs adsorbent (Fig. 2b) shows a more contrasting
215 morphology and the presence of granules with smaller size and in the form of
216 agglomerate. This is supported by elemental constituent data obtained in EDX spectra
217 (Fig. 2d) showing the existence of Fe elements of magnetite particles, in addition to
218 other elements (Si, O, C, and N) as found in ASN.

219 The presence of magnetite particles in the modified *Nannochloropsis* sp. algae
220 can be observed by comparing the XRD pattern between ASN and ASN-MPs (Fig. 3).
221 The presence of magnetite particles (Fe_3O_4) in ASN-MPs can be seen from the results
222 of the analysis with XRD (Fig. 3b). The XRD diffraction pattern in ASN-MPs has the
223 most intense appearance at $2\theta = 35.60°$ which corresponds to the diffraction pattern of

224 Fe_3O_4 particles [39] which does not appear in ASN (Fig. 3a). The XRD diffraction
225 pattern in ASN-MPs has a broad 2θ and lower intensity compared to Fe_3O_4, due to the
226 presence of amorphous silica matrix [35-37] and *Nannochloropsis* sp. which cause a
227 decrease in the level of material crystallization.

228 Addition of magnetite particles to ASN (Fig. 4b) results in a decrease in mean
229 and median of particle size in ASN-MPs (Fig. 4c). The mean and median of particles
230 sizes in ASN are 1.55 and 1.65 μm and in ASN-MPs are 1.40 and 1.53 μm, respectively.
231 This shows the decrease in particle size after coating with Fe_3O_4 particles. In Fig. 4,
232 it can be observed that there is a decrease in volume (%) for large particle size diameters
233 from 12.92 in ASN to 11.70% in AS-MPs and an increase in volume (%) in small
234 particle size from 3.50 in ASN to 4.73% in AS-MPs. These data are in line with the
235 results of observations on the surface morphology of adsorbents with SEM, as
236 previously discussed, that the presence of Fe_3O_4 particles in ASN-MPs produces
237 material with a relatively smaller particle size [9].

238 The adsorbent surface charge plays a significant part in determining the
239 optimal interaction between adsorbent and adsorbate, therefore the surface charge of
240 the adsorbent needs to be known in studying the sorption process. The surface charge

241 is determined by the zero point of charge (pH_{PZC}) which is specified as the point when
242 the zeta potential value has value of zero. The positive surface charge is indicated by
243 $pH < pH_{PZC}$, whereas the negative surface is shown by $pH > pH_{PZC}$ [38]. In current
244 study, the pH_{PZC} of ASN and ASN-MPs is around 7.3 and 7.4 respectively observed by
245 the method of solid addition (Fig. 5). Based on the pH_{PZc} values of the two adsorbents,
246 while the interaction pH in the collective adsorption process from ME and Cu(II) cation
247 solution was conditioned at pH 7.0. This is with consideration, when the pH of the
248 solution is below pH_{PZC}, the adsorbent will be positively charged while the ME solution
249 and Cu(II) cations under these conditions will also be positively charged, so there will
250 be a repulsion between the positive charge of the adsorbent and the adsorbate [39]. At
251 pH 7, the interaction between adsorbent and adsorbate can occur optimally due to at the
252 pH, the adsorbent surface charge tends to be neutral and will be negative while the ME
253 and Cu(II) cations solution are positively charged. At pH > 7 adsorption will tend to
254 decrease, because adsorbates such as a solution of ME and Cu (II) cations will undergo
255 hydrolysis which results in a negatively charged species. The same thing happened to
256 the adsorbent surface charge which tends to be negative because of pH > pHpzc [29,
257 40]. Thus in this condition, there will be a repulsion between the negative charge of the

adsorbent and adsorbate.

3.2. Adsorption kinetics of ME and Cu(II) cations

The impact of contact time on sorption between solution of ME and Cu(II) cations can be seen in Fig. 6 showing that the amount of ME and Cu(II) cations adsorbed on ASN-MPs tends to be greater than ASN. In addition, Fig. 6 shows that Cu(II) cations are more adsorbed than ME dyes in both ASN or ASN-MPs. This shows that Cu(II) cations dominate more adsorbed in ASN and ASN-MPs.

To better understand the adsorption performance of ME dyes and Cu(II) cations adsorbed in ASN and ASN-MPs, the adsorption kinetics model was used. Pseudo-first-order (Eq. (4)) and pseudo-second-order (Eq. (5)) kinetics [5, 10] could be applied to analyze the adsorption characteristics of ME dyes and Cu(II) cations shown in Table 1.

$$q_t = q_e(1 - e^{-k_1 t}) \tag{4}$$

$$\frac{t}{q_t} = \frac{1}{k_2 q_e^2} + \frac{1}{q_e} t \tag{5}$$

where q_t and q_e (mmol g^{-1}) are total adsorbate (ME or Cu(II) cation) adsorption capacity at certain time of t (min) and equilibrium, serially. While k_1 (min^{-1}) and k_2 ($g \cdot mmol^{-1} \cdot min^{-1}$) express the first and second order rate constants, respectively.

Table 1 describes the values from R^2 (linear correlation coefficient) of the pseudo-first and -second-order kinetics models compared, then both ME and Cu(II)

276 cations on ASN and ASN-MPs are more likely to take the pseudo-second-order kinetics
277 pattern. From the value of the pseudo second order rate constant (k_2) contained in
278 Table 1, it can be observed that the k_2 values of the ME and Cu(II) cation adsorbed on
279 ASN-MnPs are 8,979 x 10^{-3} and 9,784 x10^{-3} g mmol min^{-1}, respectively. These values
280 are greater than the ASN with k_2 values for ME and Cu(II) of 3,789 x10^{-3} and 6,955 x
281 10^{-3} g mmol min^{-1}, respectively. This shows that, the presence of Fe_3O_4 particles
282 increases the adsorption rate of ME or Cu(II) cation on ASN-MnPs. Therefore, the
283 Fe_3O_4 particle coating causes the adsorbent to be magnetic, so it tends to increase the
284 adsorption rate.

285 *3.3 Adsorption mechanism*

286 The significant section in the investigation of adsorption kinetics is the
287 adsorption mechanism, because it will give an overview of reaction happened between
288 adsorbate and adsorbent. In the process of the adsorption, the amount of adsorbed
289 adsorbate is always expected to be more adsorbed and easily released again
290 (desorption). The mechanism of adsorption between ME and Cu(II) cations is really
291 controlled by the surface characteristics of the adsorbent used [41, 42]. The
292 mechanism of adsorption to ME and Cu(II) cations on ASN-MPs was analyzed using

293 the proposal of Weber and Morris (Eq. (6)) about the intra-particle diffusion pattern
294 (IPD) [43, 44]. The IPD pattern can be utilized to study the diffusion process of targets
295 absorbed by adsorbents that can be used in simulating kinetics data [45].

296 $$q_t = k_{id} t^{0.5} + C \quad (6)$$

297 Where the rate constant of intra-particle diffusion is stated by k_{id} (mmol $g^{-1}min^{-0.5}$),
298 and a constant describing resistance for mass transfer in the border layer is represented
299 by C (mmol g^{-1}). Through the slope and intercept of lines resulted from plots of q_t
300 versus $t^{0.5}$ will be produced k_{id} and C (Fig. 7) and displayed in Table 2.

301 Fig. 7 describes two linear parts occurred for all plots. This model indicates
302 that involvement of the adsorption models is more than one model. The external mass
303 transfer occurs at the first linear section in the adsorption period of 0–60 minutes. The
304 diffusion of intraparticle is indicated at the second linear section in the adsorption
305 period of 60-120 minutes. The origin ($C \neq 0$) does not traversed by the second linear
306 part, this shows that the rate and external mass transfer is not controlled only by the
307 intraparticle diffusion but also it occurs simultaneously [43]. Based on observations
308 in Fig. 7, there are two steps that represent the migration of ME and Cu(II) cations
309 through the solution into the adsorbent external surface and further directed diffusion

310 through the adsorbate target into the adsorbent active site respectively through the pore
311 cavity and the adsorbent active group, according to diffusion theory at adsorption
312 process. The mechanism of adsorption may be illustrated in two dissimilar means
313 namely an electrostatic adsorption and a diffusion. This is because of the porosity and
314 existence of negative charge in the functional groups of adsorbents [39]. This is
315 supported by determining the mechanism of adsorption of ME and Cu(II) cations
316 through sequential desorption using several eluents such as distilled water, HCl solution,
317 and Na_2EDTA to release ME and Cu(II) cations which have been adsorbed on ASN-
318 MPs through entrapment interactions, electrostatic interaction, and complex formation
319 (Fig. 8).

320 In Fig. 8 can be seen the results of sequential desorption of ME dye and Cu(II)
321 cations contained in ASN-MPs by using an aquades eluent, HCl (0.1 M), and continued
322 with Na_2EDTA (0.1 M). Fig. 8 indicates that the percentage of ME dye and Cu(II)
323 cations eluted using 0.1 M HCl is greater than elution using water and 0.1 M Na_2EDTA
324 solution. This indicates that both ME and Cu(II) solutions adsorbed on ASN-MPs
325 tend to be dominated by electrostatic interactions. ME is an organic cation and Cu(II)
326 cation is positively charged so that it can interact with ASN-MPs which has a negatively

charged surface. ASN-MPs tend to be negatively charged because they have functional groups consisting of hydroxyl, carbonyl, and amines from *Nannochloropsis* sp.. Whereas siloxan and silanol groups are from silica matrix.

3.4. Adsorption isotherm

The simultaneous competition for adsorption of ME and Cu(II) cations with varying initial concentrations of ASN and ASN-MPs can be seen in Fig. 9. The results illustrate that the amount of adsorbate adsorbed goes up with rising initial concentration of adsorbate used. In fact, at the use of high initial concentrations, the amount of adsorbate adsorbed reaches a maximum. In other words, increasing the concentration does not increase the amount of adsorbate adsorbed. This is due to a decrease in the quantity of available active sites accompanied by increasing the concentration of the ME solution and the adsorbed Cu(II) cations. The sorption capacity raises caused by an enhancement in the initial concentration of ME dyes and Cu(II) cations as a booster to increase the adsorption capacity because in this condition there are more adsorbates which occupy the active sites on the adsorbent surface [46].

Fig. 9 states that the q_e value for Cu(II) cations is greater than that of ME in both ASN and ASN-MPs at the same initial concentration. In addition, it can also be seen that the q_e value of ASN-MPs adsorbents is relatively higher for ME and Cu(II) cations than ASN adsorbent. The data contained in Fig. 9 were analyzed using the Langmuir (Eq. (7)) and Freundlich (Eq. (8)) adsorption isotherm model with the assumption that

the adsorption between ME and Cu(II) cation does not influence each other in competing to occupy adsorbent active sites [47,48].

$$q_e = q_m \frac{K_L C_e}{1 + K_L C_e} \quad (7)$$

$$q_e = K_F C_e^{1/n} \quad (8)$$

where q_e and C_e represent the amount of adsorbed adsorbate per unit weight of adsorbent (mmol g^{-1}) and unadsorbed adsorbate concentration in solution at equilibrium (mmol L^{-1}), respectively. K_L and K_F are the Langmuir constant and Freundlich constant, serially.

Furthermore, the simultaneous adsorption of ME dyes and Cu(II) cation in a bi-component system was analyzed using the Langmuir isotherm equation for a binary mixture (Eq. (9)) [5, 49, 50]. The multi-component Langmuir model was the most frequently used to fit the binary biosorption data. The mathematical expression that represents the model of the Langmuir isotherm for a binary mixture can be written as follows:

$$q_{e1}^* = \frac{q_m C_{e1}^* b_1}{1 + b_1 C_{e1}^* + b_2 C_{e2}^*} \quad (9)$$

where q_m is Langmuir constant related to the capacity of adsorption, b_1 (ME) dan b_2 (Cu(II) cation) are the binary Langmuir isotherm constants. These values are

364 determined using a multiple linear regression equation as displayed in Fig. 11.

365 The analysis results of the adsorption data using Langmuir and Freundlich
366 adsorption isotherm models can be seen in Table 3. While the analysis using the binary
367 Langmuir isotherm constants model can be seen in Fig.11 and Table 4. In Table 3 and
368 Fig. 10 show that the R^2 indicates that the adsorption isotherm pattern of ME is more
369 likely to attend the Freundlich adsorption isotherm. Adsorption of ME dyes on ASN
370 and ASN-MPs goes on multiform faces of multilayer adsorbents *via* physical
371 interactions [49-51]. Adsorption of Cu(II) cations trend to take the Langmuir
372 adsorption isotherm showing that the interaction of Cu(II) cations to adsorbents is a
373 chemical interaction.

374 The Langmuir isotherm assumes that each site of active adsorption and
375 adsorbate binding ability is equivalent and does not depend on the adjacent site being
376 occupied or not. This assumption shows that adsorption occurs in the surface layer of
377 the adsorbent monolayer, after distributing the adsorption energy evenly to the entire
378 surface [52-53].

379 From the data presented in Table 4, it can be observed that the q_m values for
380 the bi-component mixture of ME dyes and Cu(II) cation in ASN and ASN-MPs are

381 1.385 x 10^{-1} and 5.319 x 10^{-1} mmolequiv g^{-1}, respectively with the binary Langmuir
382 constant isotherm $b_2 > b_1$. This shows that both the q_m value and the adsorption
383 isotherm constant from the analysis results with the binary Langmuir model (bi-
384 component system) are in line with the results obtained from the Langmuir adsorption
385 isotherm model (mono-component). From the results of data analysis using the
386 Langmuir adsorption isotherm model in the form of mono-component and bi-
387 component at the simultaneous adsorption of ME and Cu(II) cations in ASN-MPs, it
388 may be assumed that Cu(II) cations have a greater adsorption capacity (Tables 3 and 4).
389 This shows that the active groups in adsorbents derived from algal biomass (hydroxyl,
390 carbonyl, and amines groups) and silica matrix (siloxan and silanol groups) as well as
391 the magnetic properties of adsorbents can raise the quantity of available active sites on
392 the adsorbent [9,10,31]. The Cu(II) cations are more easily adsorbed by ASN-MPs
393 because Cu(II) cations have a smaller size (hydrated cation size (1.96 Å)) [54]
394 compared to ME which is a molecule with a greater size.
395 If the adsorption system assumes that there is no competition between ME
396 and Cu(II) cation as in a mono-component system. Adsorption of ME and Cu(II)
397 cation by the ASN-MPs adsorbent results q_m values of 2.915 x 10^{-1} mmol g^{-1} (93.236

398 mg g^{-1}) and 8.772 x 10^{-1} mmol g^{-1} (55.702 mg g^{-1}) (Table 3), respectively. When the
399 q_m value is compared with other adsorbents such as carbon-based adsorbents, including
400 multi-wall carbon nanotubes as ME adsorbents with q_m value of 48.06 mg g^{-1} [38] and
401 HNO_3-modified CNTs which adsorb Cu(II) cation with q_m value of 28.49 mg g^{-1} [55].
402 In addition, it can be stated that the adsorbent derived from the modified algal biomass
403 of *Nannochloropsis* sp.-silica-magnetite has a greater capacity in a bi-component
404 system. The presence of magnetite particles causes the adsorbent to be magnetic
405 thereby increasing its attraction to the adsorbate [9,11].

406 *3.5. Reuse of adsorbents*

407 The study of the ability to reuse adsorbents is one of the important parameters
408 that needs to be determined to investigate the effectiveness of repeated use of
409 adsorbents applied in the process of adsorption.

410 In this work, reuse of ASN-MPs adsorbents was carried out through an
411 adsorption-desorption process of 5 repetitions of ME and Cu(II) cations (Fig. 12). The
412 sorption results of ME and Cu(II) cations were released using distilled water and
413 continued with solution of HCl (0.1 M). The HCl was effective as eluent to release ME
414 and Cu(II) cations from ASN-MPs which were adsorbed through the electrostatic

interaction mechanism. This interaction occurs through proton substitution of ME as organic cations [56] and Cu(II) cations as hydrated cations in solution. The adsorption-desorption process was carried out repeatedly 3 times and apparently it did not reduce the percentage of ME and Cu(II) cations adsorbed significantly (Fig. 12). The percentage of ME and Cu(II) cations adsorbed began to decrease at the 4^{th} adsorption repetition, this was caused by the reduction of the adsorbent active sites due to the desorption process and adsorbent washing.

4. Conclusions

Adsorbent production from *Nannochloropsis* sp. algae biomass modified by silica matrix and magnetite particle coating has been successfully carried out. The application of ASN-MPs adsorbents on the simultaneous adsorption of solution pair of ME and Cu(II) cations with the bacth method shows that Cu(II) cations are more adsorbed than ME in simultaneous adsorption which is dominated by electrostatic interaction mechanism. ASN-MPs adsorbent is very effective in absorbing ME and Cu(II) cations in solution and it can be used up to 3 times the adsorption repetition without a significant reduction in adsorption capacity. Thus, this adsorbent can be applied for the absorption of cation mixtures of organic dyes and heavy metals that are

cationic in solutions derived from industrial waste.

Declarations

Availability of data and materials

The datasets generated during and/or analyzed during the current study are available from the corresponding author on reasonable request.

Competing interests

The authors declare they have no competing interests.

Funding

This work was funded by Ministry of Research and Technology/National Innovation and Research Agency (Kemenristek/BRIN) of the Republic of Indonesia with contract number: 179/SP2H/AMD/LT/DPRM/2020.

Authors' contributions

The manuscript was mainly based on a draft written by Buhani and Suharso, and written through contributions of all authors. All authors read and approved the final manuscript.

Acknowledgement

Ministry of Research and Technology/National Innovation and Research Agency

(Kemenristek/BRIN) of the Republic of Indonesia has funded this project with contract number: 179/SP2H/AMD/LT/DPRM/2020. Technical Service Unit of the Integrated Laboratory and the Technology Innovation Center–University of Lampung (UPT Laboratorium Terpadu dan Sentra Inovasi Teknologi–Universitas Lampung) also has provided the instruments to be used in this project.

Authors' information (optional)

References

1. Al-Saydeh SA, El-Naas MH, Zaidi SJ. Copper removal from industrial wastewater: A comprehensive review, J Ind Eng Chem. 2017; 56:35–44.
2. Guler UA, Ersan M, Tuncel E, Dugenci F. Mono and simultaneous removal of crystal violet and safranin dyes from aqueous solutions by HDTMA-modified *Spirulina* sp. Process Saf Environ. 2016;99:194-206.
3. Jamwal HS, Kumari S, Chauhan GS, Reddy NS, Ahn JH. Silica-polymer hybrid materials as methylene blue adsorbents. J Environ Chem Eng. 2017;5:103-13.
4. Holkar CR, Jadhav AJ, Pinjari DV, Mahamuni NM, Pandit AB. A critical review on textile wastewater treatments: possible approaches. J Environ Manag. 2016;182:351–66.

5. Singh N and Balomajumder C. Simultaneous removal of phenol and cyanide from aqueous solution by adsorption onto surface modified activated carbon prepared from coconut shell. J. Water Process Eng. 2016;9:233-45.

6. Wong KT, Yoon Y. Snyder SA, Jang M. Phenyl-functionalized magnetic palm-based powdered activated carbon for the effective removal of selected pharmaceutical and endocrine-disruptive compounds. Chemosphere. 2016; 152:71–80.

7. Dong Y, Liu J, Sui M, Qu Y, Ambuchi JJ, Wang H, Feng Y. A combined microbial desalination cell and electrodialysis system for copper-containing wastewater treatment and high-salinity-water desalination. J. Hazard Mater. 2017;321:307-15.

8. Kanakaraju D, Ravichandar S, Lim YC. Combined effects of adsorption and photocatalysis by hybrid TiO_2/ZnO-calcium alginate beads for the removal of copper. J Environ Sci. 2017;55:214-23.

9. Buhani, Hariyanti F, Suharso, Rinawati, Sumadi. Magnetized algae-silica hybrid from *Porphyridium* sp. biomass with Fe_3O_4 particle and its application as adsorbent for the removal of methylene blue from aqueous solution. Desalin

Water Treat. 2019;142:331-40.

10. Buhani, Musrifatun, Pratama DS, Suharso, Rinawati. Modification of *Chaetoceros* sp. biomass with silica-magnetite coating and adsorption studies towards Cu(II) ions in single and binary system. Asian J Chem. 2017;29:2734-8.

11. Buhani, Rinawati, Suharso, Yuliasari DP, Yuwono SD. Removal of Ni(II), Cu(II), and Zn(II) ions from aqueous solution using *Tetraselmis* sp. biomass modified with silica-coated magnetite nanoparticle. Desalin Water Treat. 2017;80:203–13.

12. Vijayaraghavan K, Sathishkumar M, Balasubramanian R. Interaction of rare earth elements with a brown marine alga in multi-componen solutions, Desalination. 2011;265:54-59.

13. Montazer-Rahmati MM, Rabbani P, Abdolali A, Keshtkar AR. Kinetics and equilibrium studies on biosorption of cadmium, lead, and nickel ions from aqueous solutions by intact and chemically modified brown algae. J Hazard Mater. 2011;185:401-7.

14. Angelova R, Baldikova E, Pospiskova K, Maderova Z, Safarikova M, Safarik I. Magnetically modified *Sargassum horneri* biomass as an adsorbent for organic dye removal. J Clean Prod. 2016; 137: 189-94.

15. Daneshvar E, Vazirzadeh A, Niazi A, Kousha M, Naushad M, Bhatnagar A. Desorption of Methylene blue dye from brown macro alga: Effects of operating parameters, isotherm study and kinetic modeling, J Clean Prod. 2017;152:443-53.

16. Buhani, Suharso, Satria H. Hybridization of *Nannochloropsis* sp. biomass-silica through sol-gel process to adsorb Cd(II) ion in aqueous solutions. Eur J Sci Res. 2011;51(4):467–76.

17. Flores-Chaparro CE, Ruiz LFC, de la Torre MCA, Huerta-Diaz MA, Rangel-Mendez JR. Biosorption removal of benzene and toluene by three dried macro algae at different ionic strength and temperatures: Algae biochemical composition and kinetics. J Environ Manage. 2017;193:126-35.

18. Sayadi MH, Salmani N, Heidari A, Rezaei MR. Bio-synthesis of palladium nanoparticle using *Spirulina platensis* alga extract and its application as adsorbent. Surf Interfaces. 2018;10:136–43.

516 19. Sarwa P and Verma SK. Decolourization of Orange G dye by microalgae
517 *Acutodesmus obliques* Strain PSV2 isolated from textile industrial site. Int J
518 Appl Sci Biotechnol. 2013;1(4):247–52.
519 20. Harris PO and Ramelow GJ. Binding of metal ions by particulate biomass
520 derived from *Chorella vulgaris* and *Scenedesmus quadricauda.* Environt Sci
521 Technol. 1990; 24: 220-28.
522 21. Kayan A, Arican MO, Boz Y, Ay U, Bozbas SK. Novel tyrosine-containing
523 inorganic-organic hybrid adsorbent in removal of heavy metal ions. J Env Chem
524 Eng. 2014;2:935-42.
525 22. Bozbas SK, Ay U, Kayan A. Novel inorganic-organic hybrid polymers to
526 remove heavy metals from aqueous solution, Desalin Water Treat.
527 2013;51;7208-15.
528 23. Jin X, Yu C, Li Y, Qi Y, Yang L, Zhao G, Hu H. Preparation of novel nano–
529 adsorbent based on organic−inorganic hybrid and their adsorption for heavy
530 metals and organic pollutants presented in water environment. J Hazard Mater.
531 2011;186:1672− 80.

532 24. Lee KE, Morad N, Teng TT, Poh BT. Preparation, characterization and
533 application of Mg(OH)2–PAM inorganic–organic composite polymer in
534 removing reactive dye. Iranica J Energy Environ. 2012;3:37–42.
535 25. Buhani, Suharso, Aditiya I, Kausar RA, Sumadi, Rinawati, Production of a
536 Spirulina sp. algae hybrid with a silica matrix as an effective adsorbent to absorb
537 crystal violet and methylene blue in a solution, Sustain Environ Res. 2019;29:27.
538 26. Desimone MF, He´ lary C, Mosser G, Giraud-Guille MM, Livage J, Coradin T.
539 Fibroblast encapsulation in hybrid silica/collagen hydrogels. J Mat Chem.
540 2010;20:666-8.
541 27. Tuttolomondo MV, Alvarez GS, Desimone MF, Diaz LE. Removal of azo dyes
542 from water by sol–gel immobilized *Pseudomonas* sp. J Environ Chem Eng.
543 2014;2:131–6.
544 28. Martins LR, Rodrigues JAV, Adarme OFH, Melo TMS, Gurgel LVA, Gil
545 LF. Optimization of cellulose and sugarcane bagasse oxidation: Application for
546 adsorptive removal of crystal violet and auramine-O from aqueous solution. J
547 Colloid Interface Sci. 2017;494:223-41.

548 29. Lin Y, Chen H, Lin K, Chen B, Chiou C. Application of magnetic modified with
549 amino groups to adsorb copper ion in aqueous solution. J Environ Sci.
550 2011;23:44-50.
551 30. Peng Q, Liu Y, Zeng G, Xu W, Yang C, Zhang J. Biosorption of copper(II) by
552 immobilizing *Saccharomycescerevisiae* on the surface of chitosan-coated
553 magnetic nanoparticle from aqueous solution. J Hazard Mater. 2010;177:676-
554 82.
555 31. Ghosh S, Badruddoza AZM, Hidajat K, Uddin MS. Adsorptive removal of
556 emerging contaminants from water using superparamagnetic Fe_3O_4
557 nanoparticles bearing aminated ß-cyclodextrin. J Environ Chem Eng.
558 2013;1:122–30.
559 32. Araghi SH, Entezari MH. Amino-functionalized silica magnetite nanoparticles
560 for the simultaneous removal of pollutants from aqueous solution. Appl Surf
561 Sci. 2015;333:68-77.
562 33. Anirudhan TS, Shainy F, Adsorption behaviour of 2-mercaptobenzamide
563 modified itaconic acid-grafted-magnetite nanocellulose composite for
564 cadmium(II) from aqueous solutions. J Ind Eng Chem. 2015;32:157–66.

565 34. Wondracek MHP, Jorgetto AO, Silva ACP, Ivassechen JR, Schneider JF, Saeki
566 MJ, Pedrosa VA, Yoshito WK, Colauto F, Ortiz WA, Castro GR. Synthesis of
567 mesoporous silica-coated magnetic nanoparticles modified with 4-amino-3-
568 hydrazino-5-mercapto-1,2,4-triazole and its application as Cu(II) adsorbent
569 from aqueous samples. *App Surf Sci.* 2016;367:533-41.
570 35. Mohmood I, Lopes CB, Lopes I, Tavares DS, Soares AMVM, Duarte AC,
571 Trindade T, Ahmad I, Pereira E. Remediation of mercury contaminated
572 saltwater with functionalized silica coated magnetite nanoparticles. Sci Total
573 Environ. 2016;557–558:712-21.
574 36. Zhang J, Zhai S, Li S, Xiao Z, Song Y, An Q, Tian G. Pb(II) removal of
575 Fe_3O_4@SiO_2–NH_2 core–shell nanomaterials prepared via a controllable sol–gel
576 process. Chem Eng J. 2013;215–216: 446-71.
577 37. Hu H, Wang Z, Pan L. Synthesis of monodisperse Fe_3O_4 @ silica core–shell
578 microspheres and their application for removal of heavy metal ions from water.
579 *J Alloys Comp.* 2010;492:656-61.

580 38. Ai L, Zhang C, Liao F, Wang Y, Li M, Meng L. Removal of methylene blue
581 from aqueous solution with magnetite loaded multi-wall carbon nanotube:
582 kinetic, isotherm and mechanism analysis. J Hazard Mater. 2011;198: 282–90.
583 39. Ebadollahzadeh H, Zabihi M, Competitive adsorption of methylene blue and Pb
584 (II) ions on the nano-magnetic activated carbon and alumina. Mater Chem Phys.
585 2020:122893.
586 40. Gupta VK, Rastogi A. Biosorption of lead from aqueous solution by green algae
587 Spirogyra species: Kinetics and equilibrium studies. J Hazard Mater.
588 2008 ;152:407-14.
589 41. Achak M, Hafidi A, Ouazzani N, Sayadi S, Mandi L. Low cost biosorbent
590 banana peel for the removal of phenolic compounds from olive mill wastewater:
591 Kinetic and equilibrium studies. J Hazard. Mater. 2009;166:117–25.
592 42. Buhani, Puspitarini M, Rahmawaty, Suharso, Rilyanti M, Sumadi, Adsorption
593 of phenol and methylene blue in solution by oil palm shell activated carbon
594 prepared by chemical activation. Orient J Chem. 2018;34(4):2043–50.
595 43. Liang YD, He YJ, Wang TT, Lei LH. Adsorptive removal of gentian violet from
596 aqueous solution using $CoFe_2O_4$//activated carbon magnetic composite. J Water

597 Process Eng. 2019;27:77-88.

598 44. AbdEl-Salam AH, Ewais HA, Basaleh AS. Silver nanoparticles immobilised on
599 the activated carbon as efficient adsorbent for removal of crystal violet dye from
600 aqueous solutions. A kinetic study. J Mol Liq. 2017 ;248:833-41.

601 45. Dogan M, Abak H, Alkan M. Adsorption of methylene blue onto hazelnut shell:
602 Kinetics, mechanism and activation parameters. J Hazard Mater. 2009;164:172–
603 81.

604 46. Zabihi M, Haghighi Asl A, Ahmadpour A, Studies on adsorption of mercury
605 from aqueous solution on activated carbons prepared from walnut shell. J.
606 Hazard. Mater. 2010;174:251–56.

607 47. Ho YS, Porter JF, McKay G. Equilibrium isotherm studies for the sorption of
608 divalent metal ions onto peat: Copper, Nickel, and Lead single component
609 systems. Water Air Soil Pollut. 2002;141:1–33.

610 48. Foroutan R, Esmaeili H, Abbasi M, Rezakazemi M, Mesbah M. Adsorption
611 behavior of Cu (II) and Co (II) using chemically modified marine algae.
612 Environ. Technol. 2018;39 (21): 2792-800.

613 49. Fagundes-Klen MR, Ferri P, Martins TD, Tavares CRG, Silva EA. Equilibrium

study of the binary mixture of cadmium–zinc ions biosorption by the *Sargassum filipendula* species using adsorption isotherms models and neural network. Biochem Eng J. 2007;34:136–46.

50. Kleinübing SJ, .da Silva EA, da Silva MGC, Guibal E. Equilibrium of Cu(II) and Ni(II) biosorption by marine alga Sargassum filipendula in a dynamic system: Competitiveness and selectivity. Bioresour Technol. 2011;102(7): 4610-17.

51. Shao Y, Zhou L, Bao C, Ma J, Liu M, Wang F. Magnetic responsive metal–organic frameworks nanosphere with core–shell structure for highly efficient removal of methylene blue. Chem Eng J. 2016;283:1127–36.

52. Xin X, Wei Q, Yang J, Yan L, Feng R, Chen G, et al. Highly efficient removal of heavy metal ions by amine-functionalized mesoporous Fe_3O_4 nanoparticles. Chem Eng J. 2012;184:132-40.

53. Larraza I, Lopez-Gonzalez M, Corrales T, Marcelo G. Hybrid materials: magnetite-Polyethylenimine-Montmorillonite, as magnetic adsorbents for Cr(VI) water treatment. J Colloid Interf Sci. 2012;385:24-33.

54. Martell AE, Hancock RD, Metal Complexes in Aqueous Solution. Plenum

631 Prsess, New York. 1996.

632 55. Li YH, Ding J, Luan Z, Di Z, Zhu Y, Xu C, Wu D, Wei B. Competitive
633 adsorption of Pb^{2+},Cu^{2+}, and Cd^{2+}ions from aqueous solutions by multiwalled
634 carbon nanotubes. Carbon 2003; 41:2787–92.

635 56. Varghese SP, Babu AT, Babu B, Antony R. γ-MnOOH nanorods: efficient
636 adsorbent for removal of methylene blue from aqueous solutions. J Water
637 Process Eng. 2017;19:1-7.

638

639

640

Figures

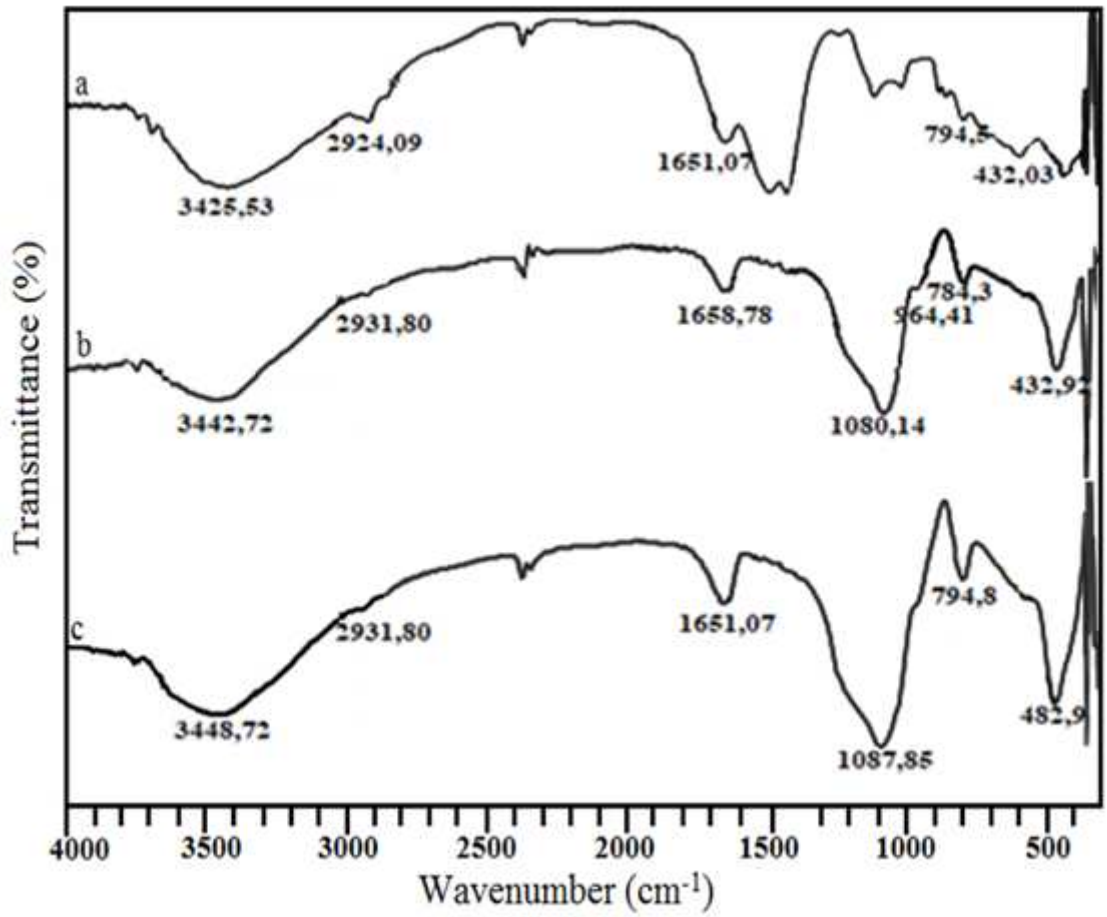

Figure 1

FTIR Spectrum of (a) Nannochloropsis sp., (b) ASN, and (c) ASN-MPs.

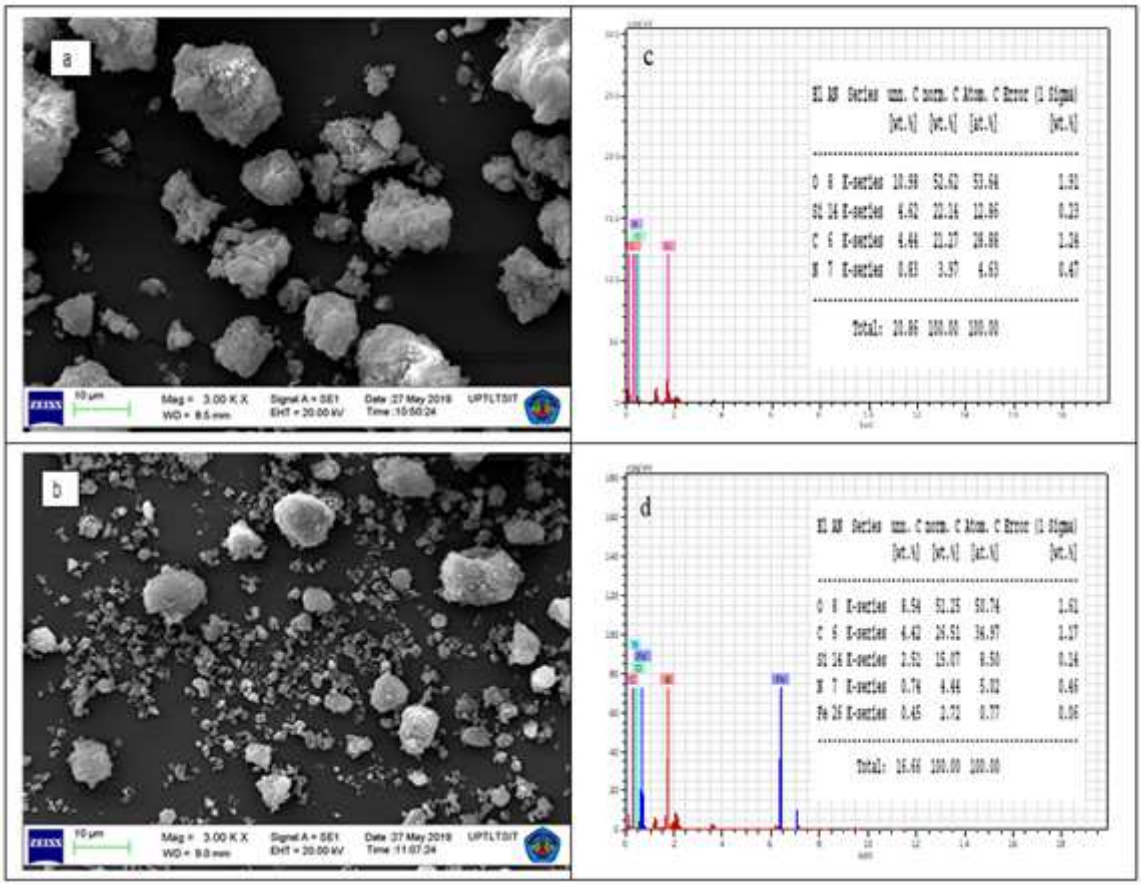

Figure 2

SEM-EDX of (a,c) ASN and (b,d) ASN-MPs

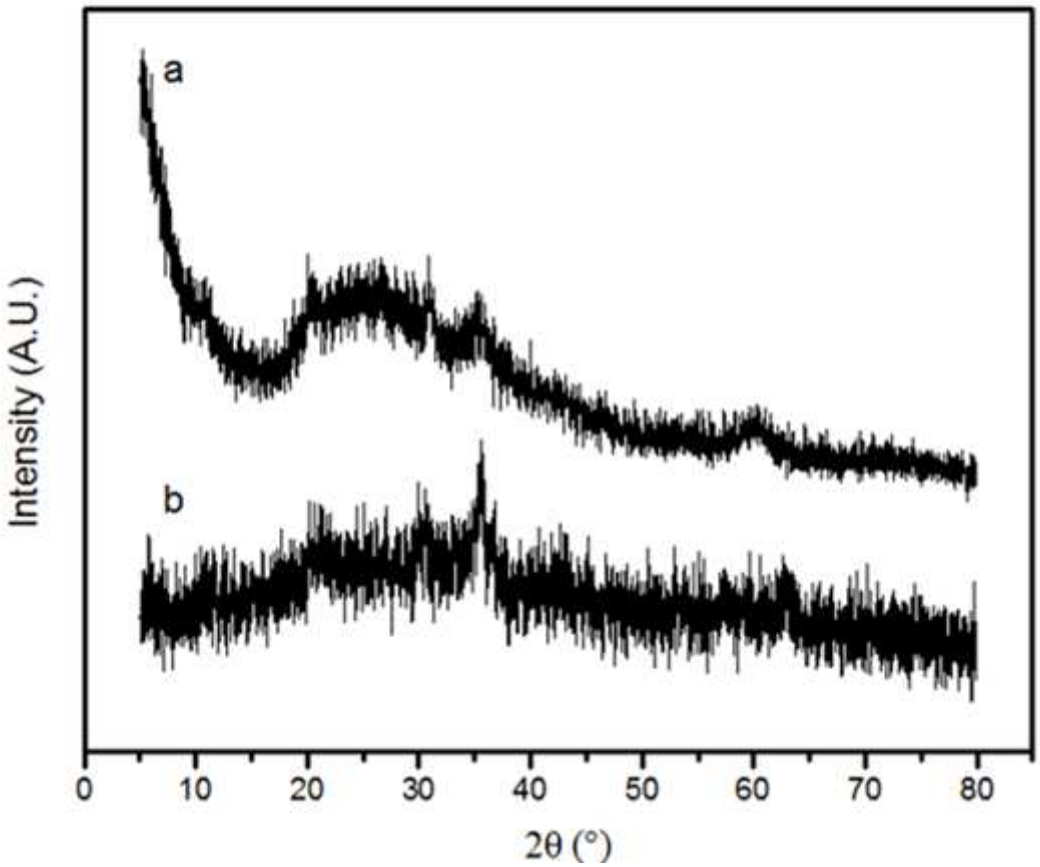

Figure 3

XRD pattern of (a) ASN and (b) ASN-MPs.

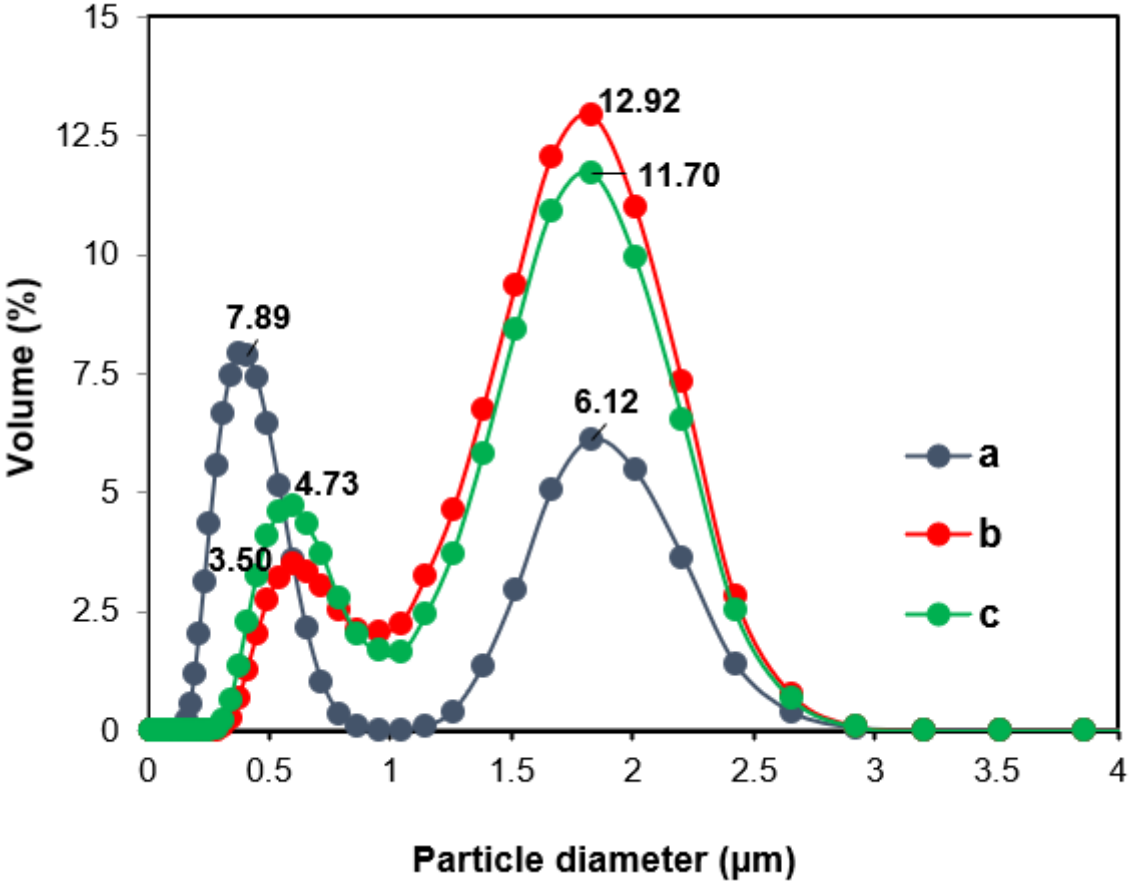

Figure 4

Particle size distribution of (a) Fe3O4, (b) ASN, and (c) ASN-MPs.

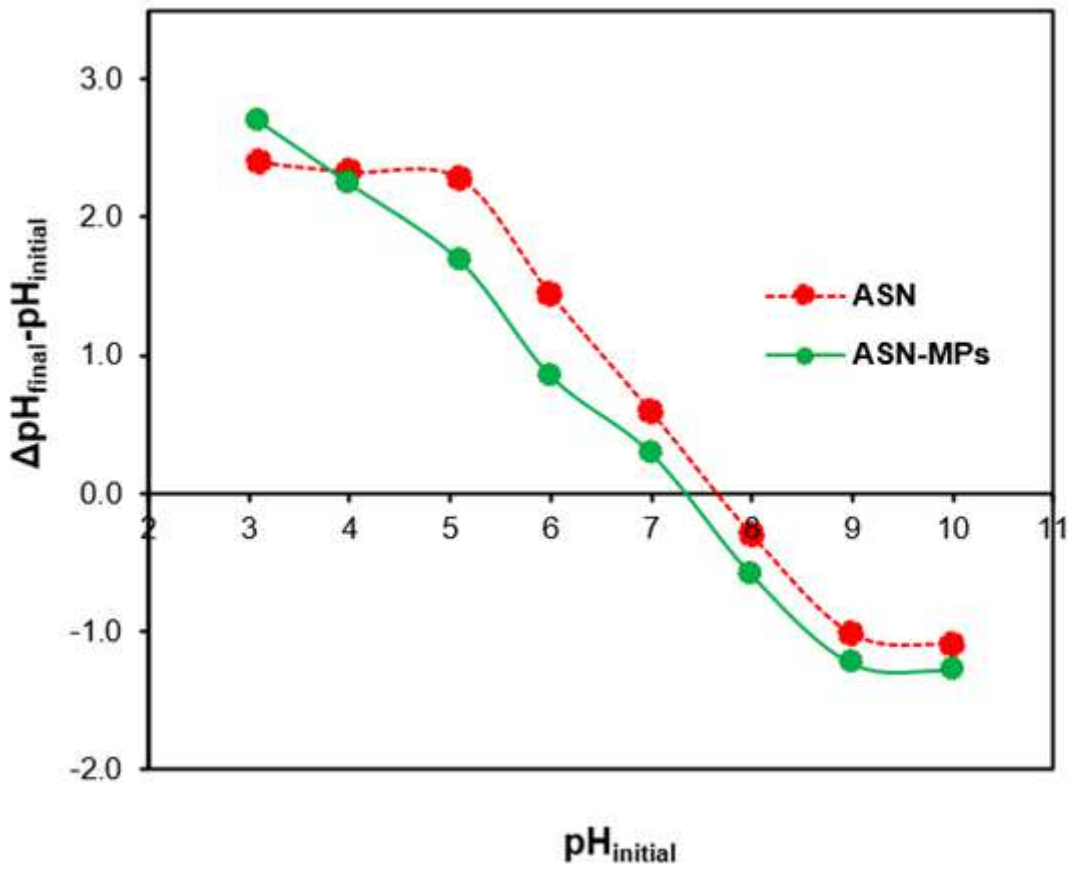

Figure 5

Determination of the point of zero charge of the ASN and ASN-MPs.

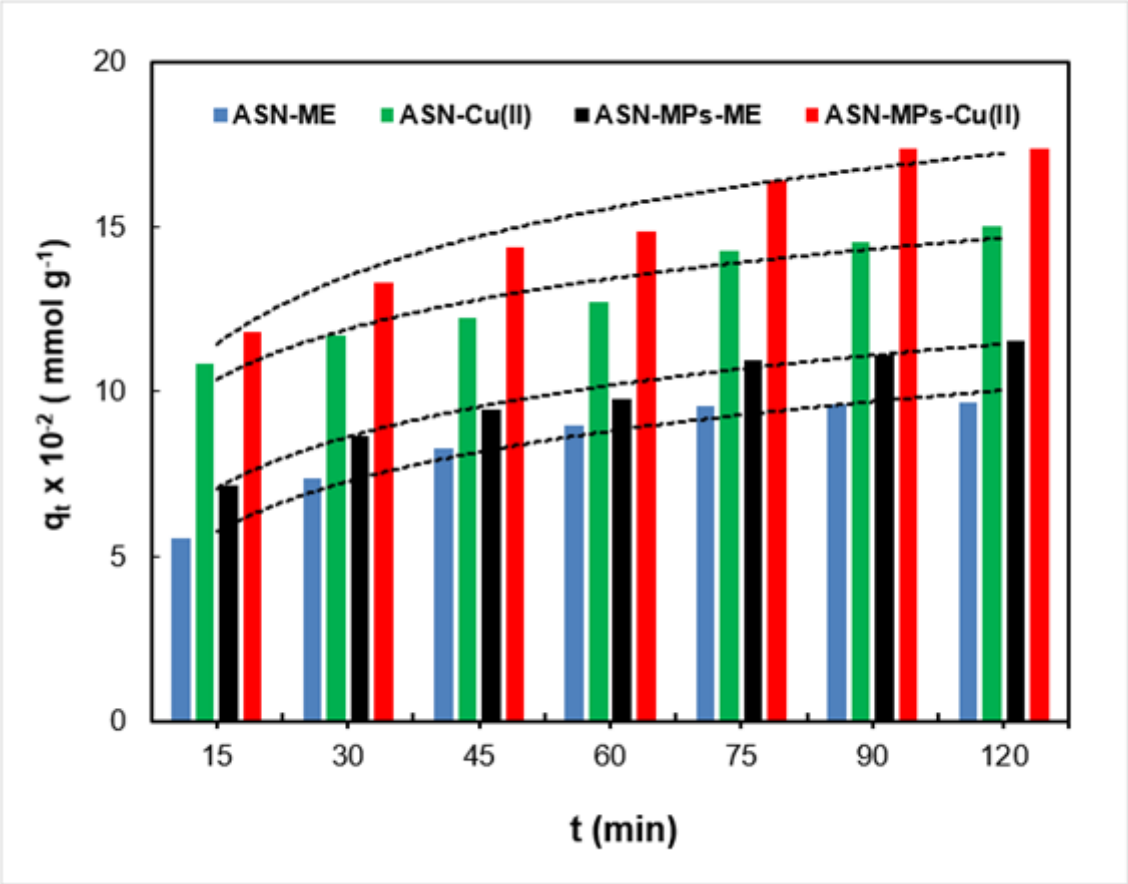

Figure 6

The relationship between interaction time and the amount of ME and Cu(II) cations adsorbed on ASN and ASN-MPs.

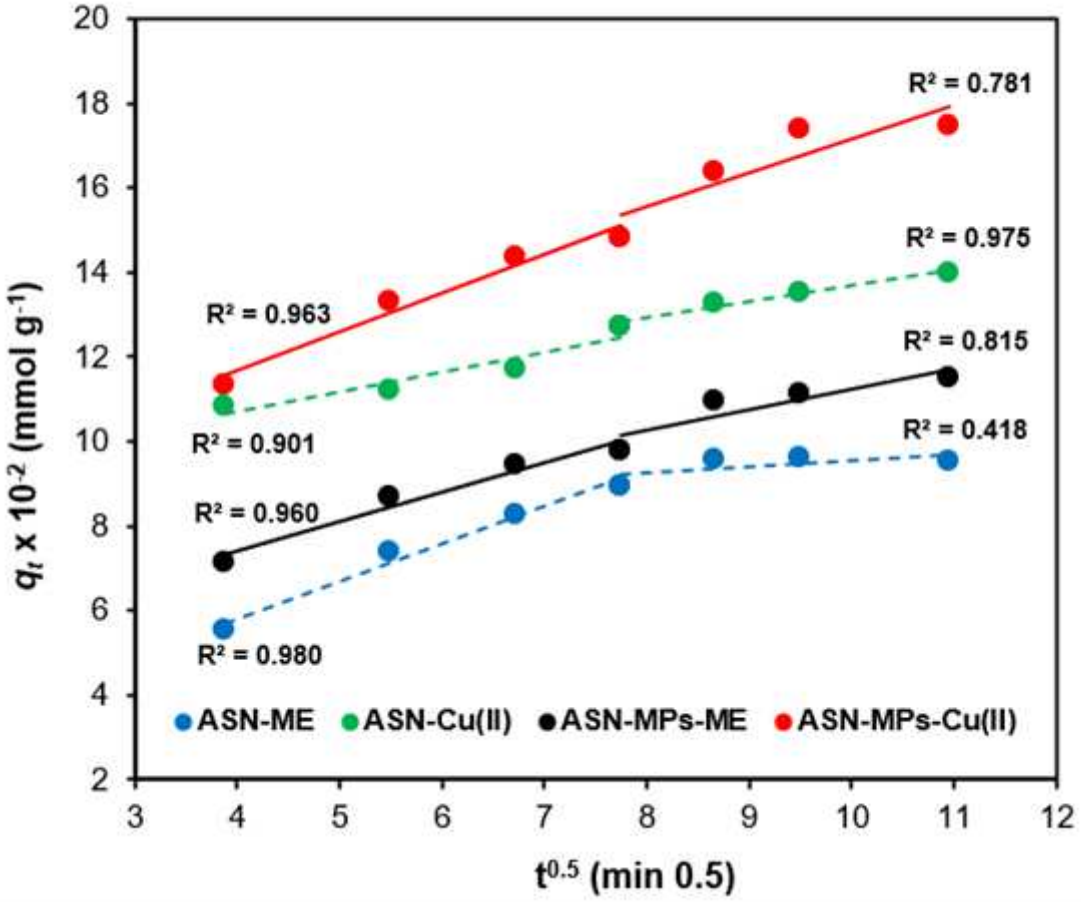

Figure 7

Intra-particle diffusion (IPD) model-predicted kinetics of ME and Cu(II) cations sorption by ASN and ASN-MPs.

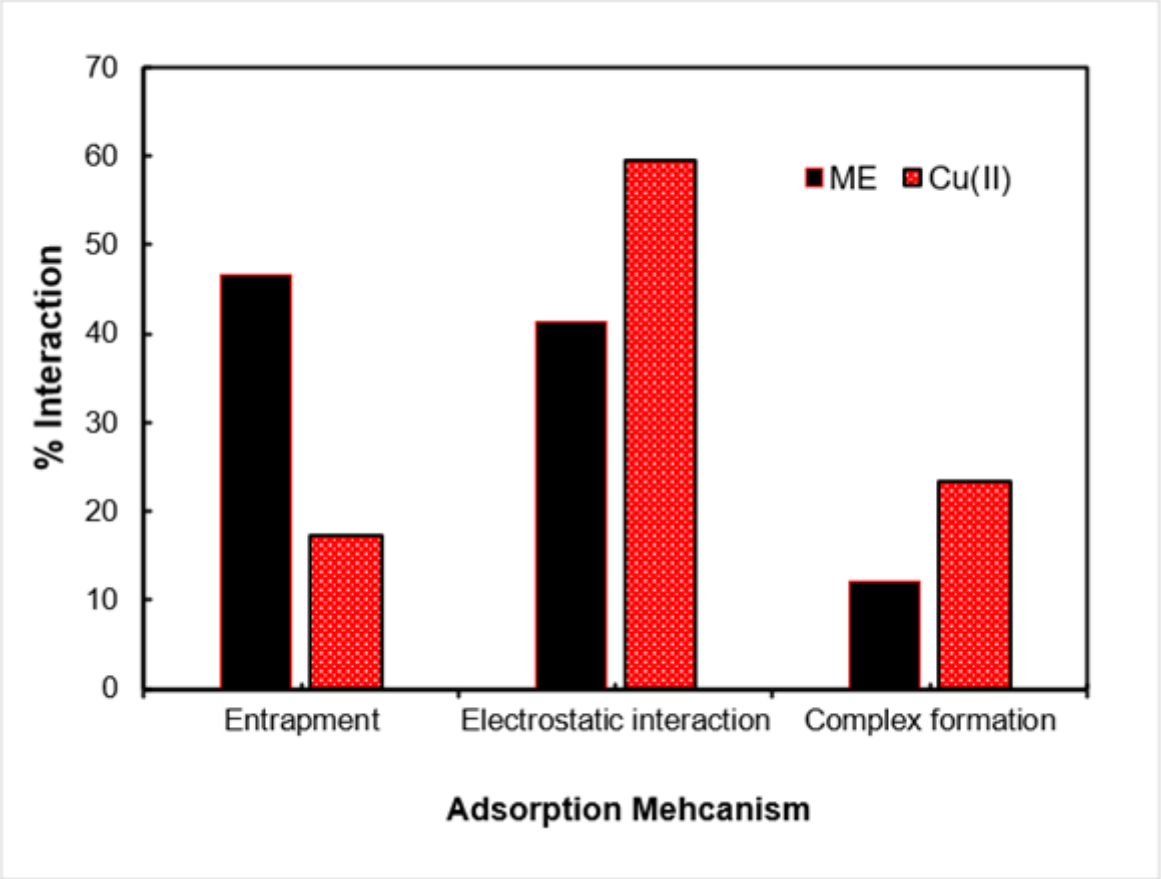

Figure 8

Contribution of the adsorption mechanism of ME and Cu(II) cations to ASN-MPs material.

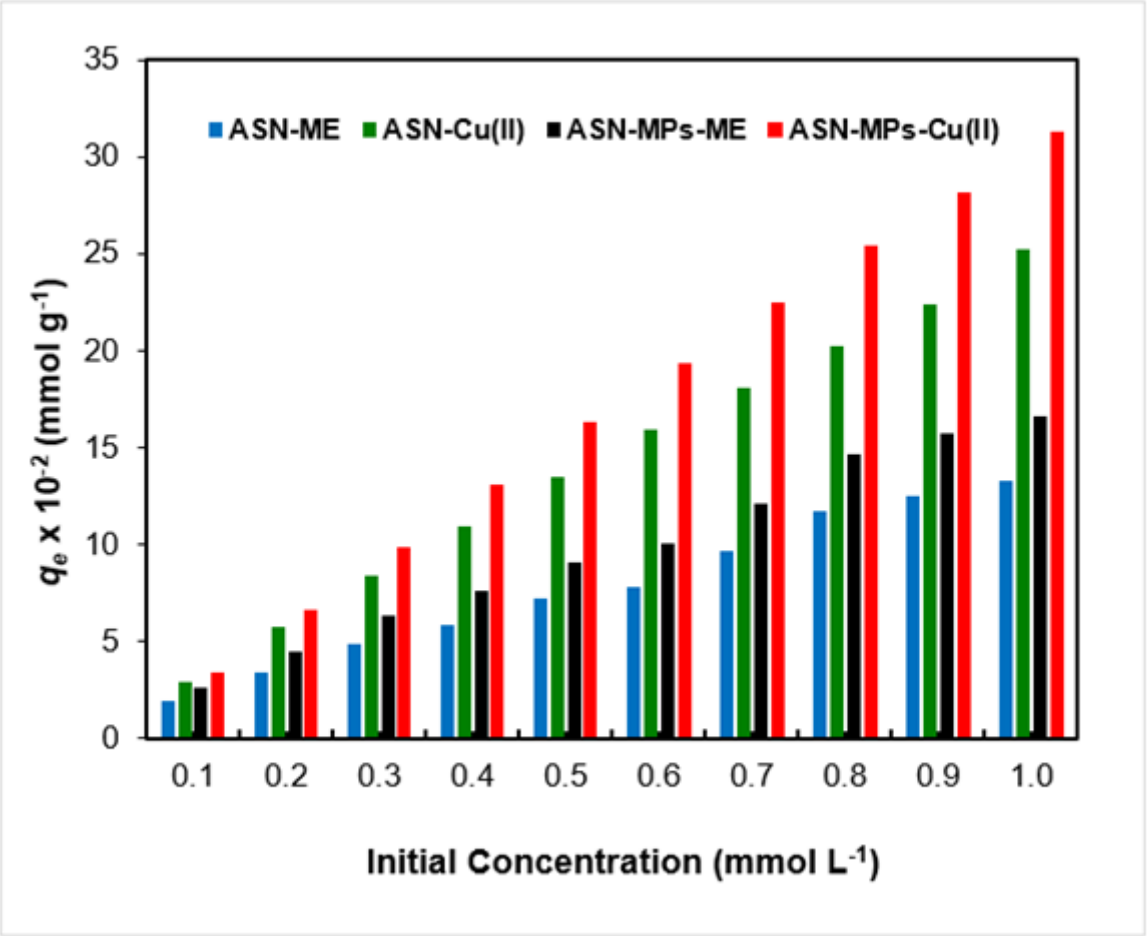

Figure 9

The relationship between interaction time and the amount of ME and Cu(II) cations adsorbed simultaneously on ASN and ASN-MPs.

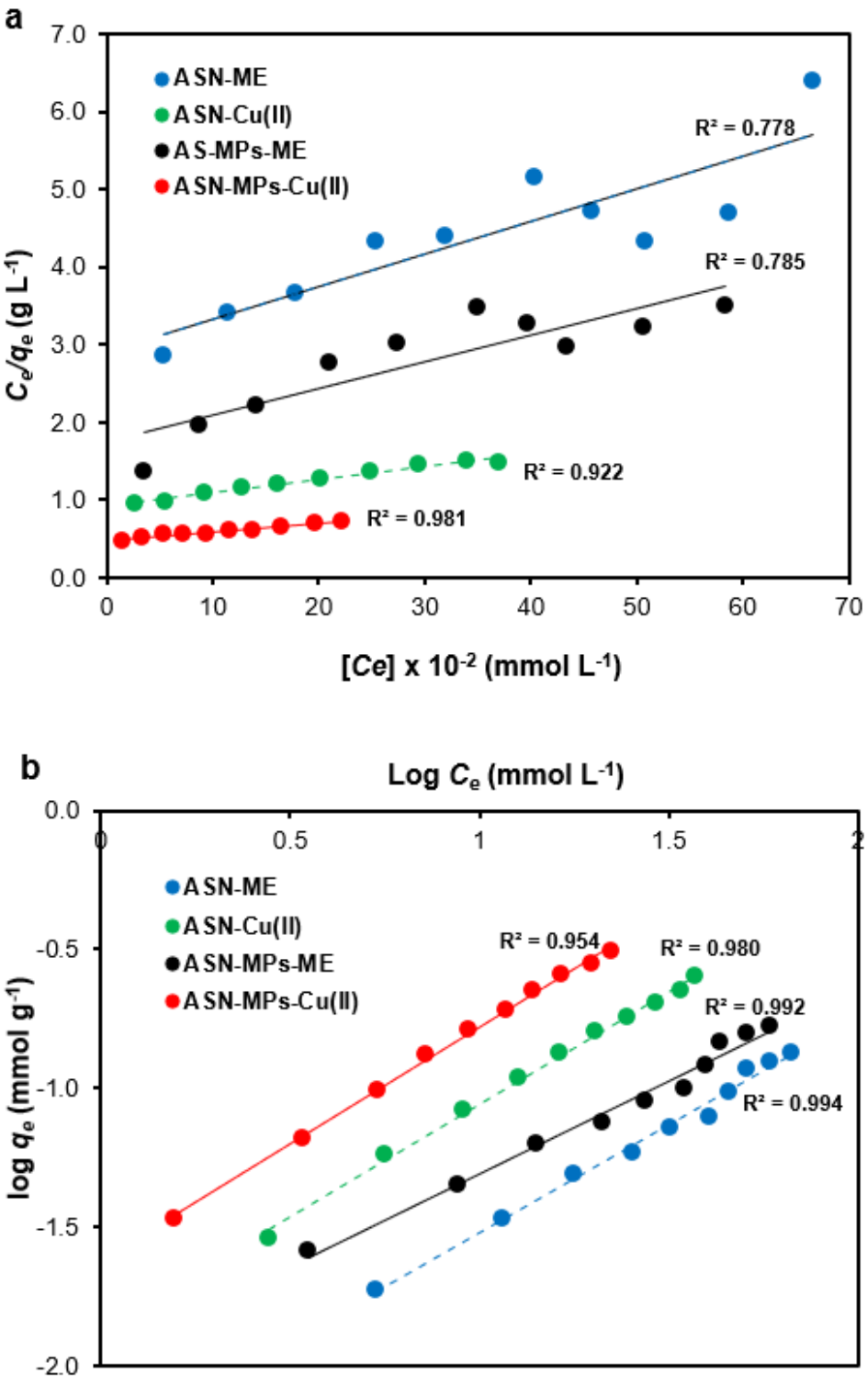

Figure 10

The liniear regression of ME and Cu(II) cations on ASN and ASN-MPs by comparing the equilibrium adsorption data with the (a) Langmuir and (b) Freundlich adsorption models.

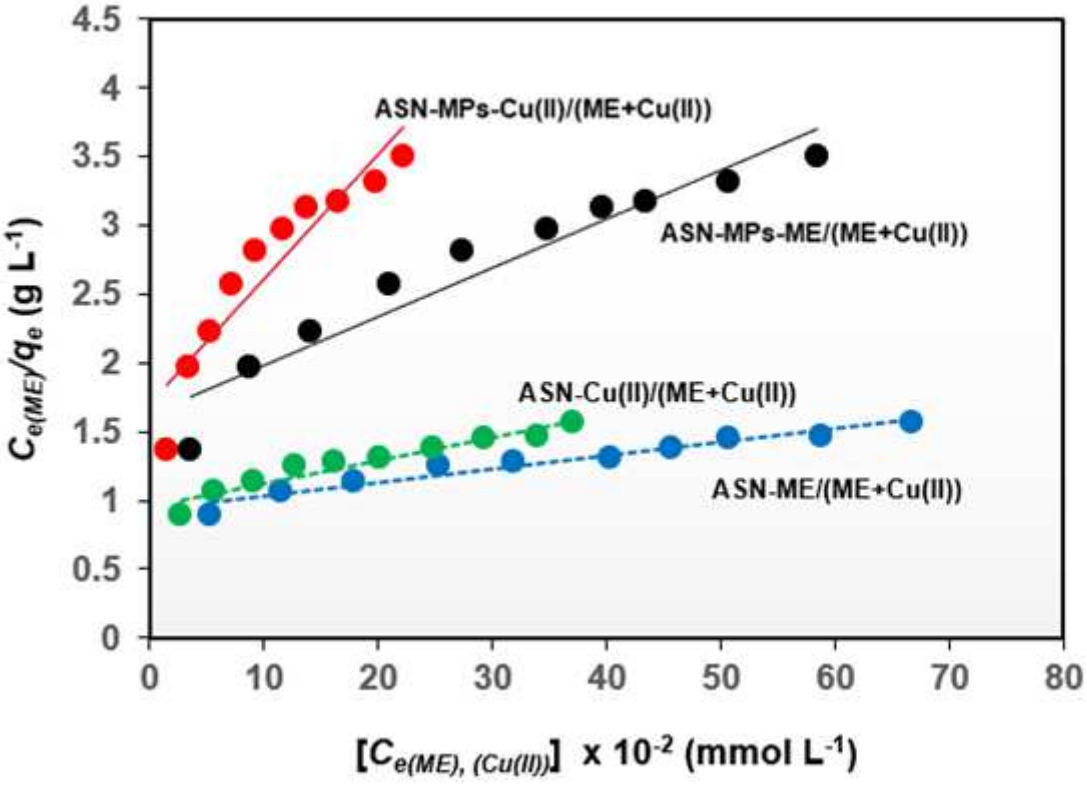

Figure 11

The Multiple linear regression of ME and Cu(II) cations on ASN and ASN-MPs by the multi-component Langmuir adsorption model.

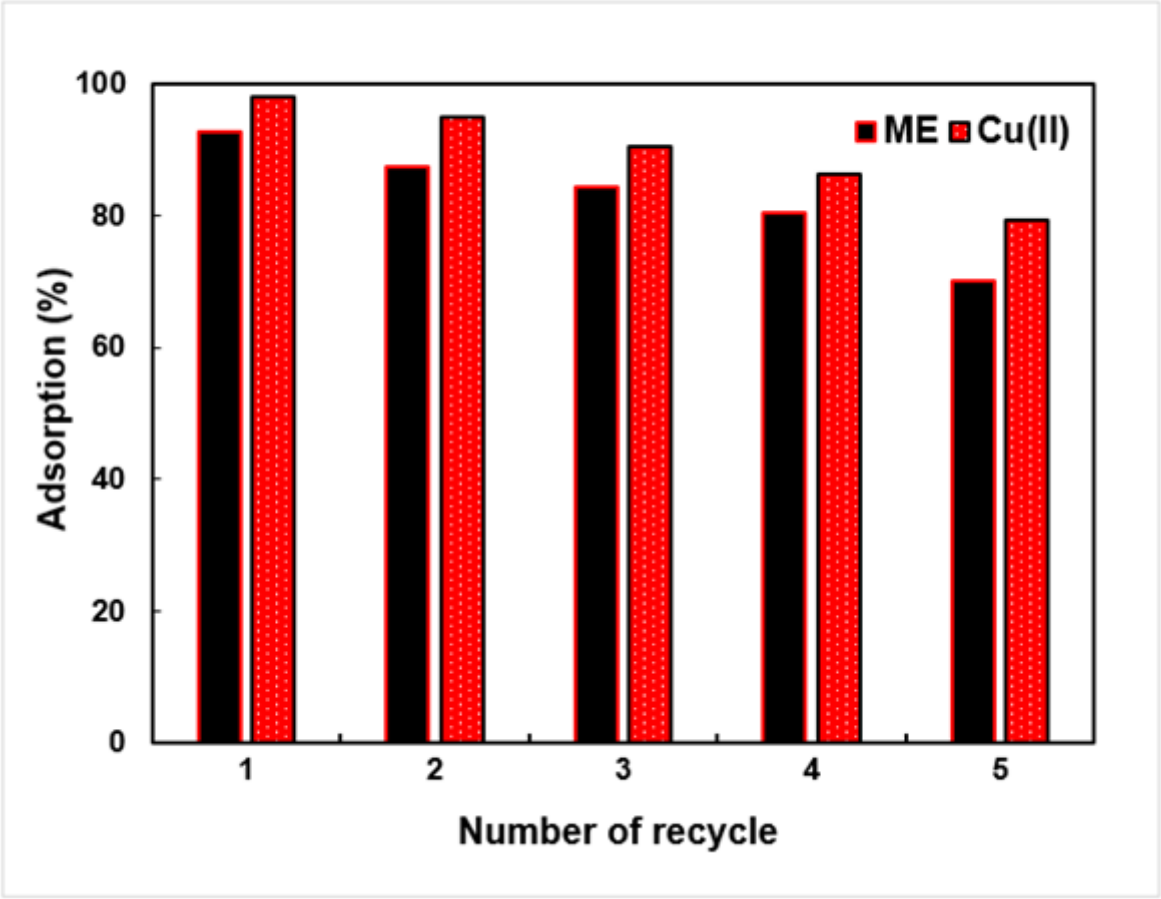

Figure 12

Reuse of AS-MPs adsorbents by ME and Cu(II) cations.